Human Molecular Genetics, 2014, Vol. 23, No. 2 **303–318**
doi:10.1093/hmg/ddt421
Advance Access published on September 5, 2013

Rescue of behavioral and EEG deficits in male and female Mecp2-deficient mice by delayed *Mecp2* gene reactivation

Min Lang[1,3], Robert G. Wither[1,3], Sinisa Colic[5], Chiping Wu[2], Philippe P. Monnier[1,3], Berj L. Bardakjian[5], Liang Zhang[2,4] and James H. Eubanks[1,3,6,*]

[1]Division of Genetics and Development and [2]Division of Fundamental Neuroscience, Toronto Western Research Institute, University Health Network, 399 Bathurst Street, Toronto, ON, Canada M5T 2S8 [3]Department of Physiology, [4]Department of Neurology, [5]Department of Electrical and Computer Engineering and [6]Department of Surgery (Neurosurgery), University of Toronto, Toronto, ON, Canada M5S 1A8

Received June 3, 2013; Revised July 29, 2013; Accepted August 27, 2013

Mutations of the X-linked gene encoding methyl CpG binding protein type 2 (*MECP2*) are the predominant cause of Rett syndrome, a severe neurodevelopmental condition that affects primarily females. Previous studies have shown that major phenotypic deficits arising from MeCP2-deficiency may be reversible, as the delayed reactivation of the *Mecp2* gene in Mecp2-deficient mice improved aspects of their Rett-like phenotype. While encouraging for prospective gene replacement treatments, it remains unclear whether additional Rett syndrome co-morbidities recapitulated in Mecp2-deficient mice will be similarly responsive to the delayed reintroduction of functional Mecp2. Here, we show that the delayed reactivation of *Mecp2* in both male and female Mecp2-deficient mice rescues established deficits in motor and anxiety-like behavior, epileptiform activity, cortical and hippocampal electroencephalogram patterning and thermoregulation. These findings indicate that neural circuitry deficits arising from the deficiency in Mecp2 are not engrained, and provide further evidence that delayed restoration of Mecp2 function can improve a wide spectrum of the Rett-like deficits recapitulated by Mecp2-deficient mice.

INTRODUCTION

Methyl-CpG-binding protein 2 (MeCP2) is a key epigenetic factor whose transcriptional regulating functions are required for the proper development and maintenance of the central nervous system (1–5). While *MECP2* mutations have been established to be the underlying cause of Rett syndrome (1), mutations and polymorphisms of *MECP2* have also been found in distinct conditions such as X-linked mental retardation, Angelmann syndrome, schizophrenia and forms of learning disability (6). Furthermore, while causality has yet to be clearly established, non-coding mutations in the 3′ untranslated region of *MECP2* have been detected in cases of attention deficit/hyperactivity disorder and autism, raising the possibility that altered MeCP2 function could also contribute to these conditions (6–8). Although the specific functions of MeCP2 that become compromised due to these specific mutations remain to be fully elucidated, it is clear that deficits in proper MeCP2 function can lead to impaired neural network function and cause pronounced neurological and behavioral phenotype impairments.

Mecp2-deficient mouse models have been generated (9–16), and collectively these models recapitulate many of the phenotypes associated with clinical *MECP2* mutations (17). Behavioral impairments, neural circuitry abnormalities, autonomic dysfunction, synaptic electrical deficits and anatomical alterations have all been reported in Mecp2-deficient mice (18–28). Due to the X-linked nature of the *Mecp2* gene, male Mecp2-deficient mice display a greater level of affectedness than heterozygous female Mecp2-deficient mice (9,10,29). Importantly, though, there is evidence to suggest that impairments resulting from the lack of Mecp2 function are not irremediable, as the reinstatement of Mecp2 expression in Mecp2-deficient mice was

*To whom correspondence should be addressed at: Mac 13-423, Toronto Western Research Institute, 399 Bathurst Street, Toronto, ON, Canada M5T 2S8. Tel: +1 4166035800; Fax: +1 4166035745; Email: jeubanks@uhnres.utoronto.ca

shown to extend lifespan, improve gross phenotypic severity and rescue deficits in local hippocampal synaptic plasticity (16). Recently, it was also demonstrated that restoring Mecp2 expression in male Mecp2-deficient mice improved respiratory function, behavioral performances and neuronal morphology (30). Despite this, the full extent of delayed phenotypic rescue following functional Mecp2 reintroduction remains unclear, as the rescue potential of several neurophysiological and behavioral impairments present in Mecp2-deficient mice that are common to Rett syndrome patients have not been fully evaluated. To address this, we reactivated *Mecp2* in both male and female symptomatic Mecp2-deficient mice and assessed the effects of delayed *Mecp2* reactivation on already established deficits in longevity, behavioral performance, neural network activity, cortical and hippocampal oscillatory patterns and thermoregulation.

RESULTS

Reactivation of *Mecp2* extends lifespan and improves the general phenotypic severity of Mecp2-deficient mice

To generate mutant mice in which functional Mecp2 expression could be reactivated conditionally, we crossed female Mecp2-deficient ($MeCP2^{+/-}$) mice containing a 'stop-flox' *Mecp2* allele (16) with transgenic mice expressing an estrogen receptor/cre-recombinase (31) transgene from the ROSA26 gene locus (32). This transgenic mouse line has been shown previously to express the estrogen receptor/cre recombinase transgene throughout the brain and body, and target both glial cells and neurons throughout the brain (32). For simplicity, we will refer to Mecp2-deficient mice or Mecp2-deficient mice expressing cre recombinase without reactivation as 'Non-Rescue' mice, and mice in which a functional *Mecp2* gene has been reactivated as 'Rescue' mice. Between postnatal days 50–70, male 'Rescue' mice were generated by intraperitoneal injections of tamoxifen (see Materials and Methods). Female 'Rescue' mice were similarly generated by tamoxifen administration, but injection times ranged from 270 to 320 days of age to allow similar levels of phenotypic severity in the female mice to develop. The relative level of Mecp2 expression in the male and female 'Non-Rescue' and 'Rescue' cohorts was assessed between 3–5 months post-*Mecp2* reactivation in males, and 5–9 months post-*Mecp2* reactivation in females by immunoblot and immunohistochemical analysis using age and gender-matched wild-type mice as references. As shown in Figure 1, Mecp2 prevalence in brains of male 'Non-Rescue' mice was 1.7 $\pm$ 1.1% of average wild-type levels. Mecp2 prevalence in the male 'Rescue' mouse brain ranged from 21.1 to 87.5 percentage of wild-type, with an average level of 52.4 $\pm$ 14.4% of wild-type Mecp2 levels (Fig. 1A and C). In female 'Non-Rescue' mice, Mecp2 levels had an overall average value of 53.3 $\pm$ 6.1% of wild-type levels. The average Mecp2 prevalence in a cohort of female 'Rescue' mice was 68.7 $\pm$ 7.3% of wild-type levels (Fig. 1B and D). Although proportionally consistent with the level of reactivation achieved in the male 'Rescue' mouse cohort, the level of Mecp2 in the group of female 'Rescue' mice examined did not statistically differ from the Mecp2 levels in female 'Non-Rescue' mice ($P = 0.08$). Interestingly, though, the overall level of Mecp2 expression in male 'Rescue' mice was comparable to that in female 'Non-Rescue' mice ($P = 0.17$), suggesting that the mosaic Mecp2 expression pattern in male 'Rescue' mice is similar in magnitude overall to that of female 'Non-Rescue' mice. Mecp2 protein expression was confirmed in male 'Rescue' mice by immunohistochemical analysis (Fig. 1E and F). As expected, immunostaining confirmed *Mecp2* reactivation throughout the brain, with prominent labeling detected within the nucleus of neurons, and lower levels present in glial cells (Fig. 1E and F).

Consistent with previous observations (9,10,12,16,30,33,34), male 'Non-Rescue' mice displayed an early lethality, with a median survival age of 67 days (Fig. 2A). In contrast, the lifespan of male 'Rescue' mice was significantly longer, displaying a median survival age of 286 days ($P < 0.01$, Fig. 2A). While not a complete rescue to wild-type, Kaplan–Meyer survival analysis revealed the lifespan plots of the male 'Rescue' mice was similar to that of female 'Non-Rescue' mice (Fig. 2A), which likely display a similar mosaic Mecp2 expression pattern. The extension of lifespan did not correspond, however, with a concomitant increase in body mass. Male 'Non-Rescue' mice weighed significantly less than male wild-type mice at all ages examined (Fig. 2B, $P < 0.01$). Although lifespan was dramatically extended, the body weight of male 'Rescue' mice remained significantly below that of wild-type mice throughout their increased lifespan. Further, at times following *Mecp2* reactivation, the average growth rate of male 'Rescue' mice remained significantly below that of male wild-type mice (0.25 g/week versus 0.88 g/week, respectively; $P < 0.01$).

The longevity of female 'Rescue' mice was also significantly extended. The median lifespan of female 'Non-Rescue' mice was found to be 356 days, and none of the female 'Non-Rescue' mice survived longer than 570 days. Ninety-two percent of the female 'Non-Rescue' mice (24 of 26) died spontaneously before 500 days of age (Fig. 2A). In contrast, none of the female 'Rescue' mice after receiving tamoxifen died spontaneously prior to 500 days of age, and the overall median lifespan of these female 'Rescue' mice was 675 days, which was significantly longer than that of female 'Non-Rescue' mice ($P < 0.05$). In fact, this median survival age was comparable to that of female wild-type mice (679 days), and Kaplan–Meyer analysis revealed no significant differences between the lifespan plots of female 'Rescue' and female wild-type mice ($P > 0.05$).

Similar to what has been previously reported (16,30), the general phenotypic severity of both male and female 'Rescue' mice was improved significantly following *Mecp2* reactivation. Using a previously validated 12-point severity scale (3,16,30,34), male 'Pre-Rescue' mice showed a phenotypic severity of 6.8 $\pm$ 0.5 at the time of tamoxifen injection, and the same cohort of mice showed a significantly lower score of 5.8 $\pm$ 0.7 at 3 months following *Mecp2* reactivation in male 'Non-Rescue' mice between 70 and 90 days of age (Fig. 2C). This comparison was required, as each of the male 'Non-Rescue' mice had died or been sacrificed due to overt morbidity at the later times of severity score assessment in the male 'Rescue' mice. A similar robust improvement was seen in female 'Rescue' mice. At the time of tamoxifen injection, female 'Pre-Rescue' mice displayed an average phenotypic severity score of 5.1 $\pm$ 0.2. At 3 months following *Mecp2* reactivation, the severity score of the same group was 3.8 $\pm$ 0.2 (Fig. 2D).

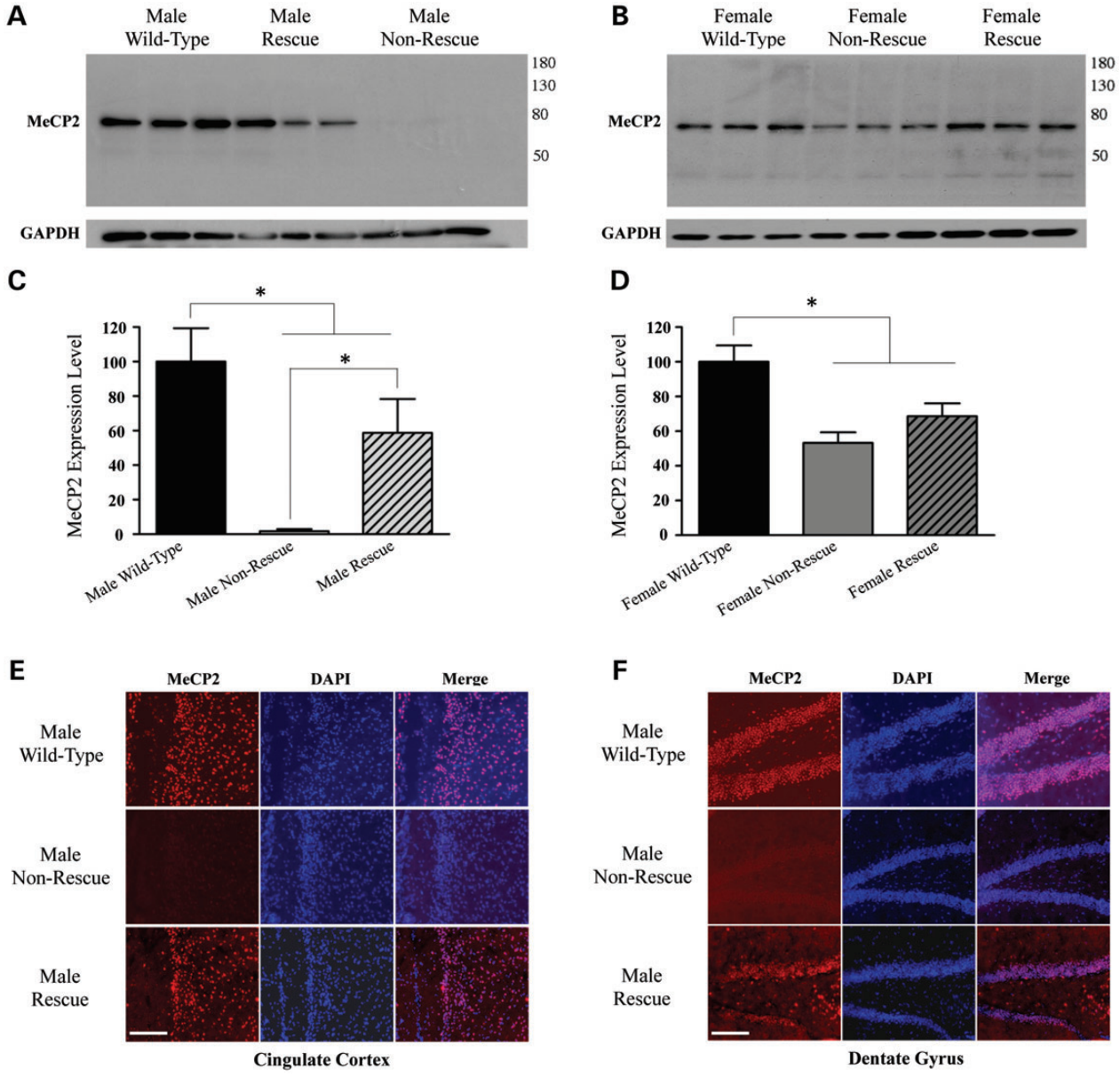

Figure 1. Mecp2 expression was restored in male and female 'Rescue' mice following tamoxifen treatment. (**A**) Representative western blot showing Mecp2 expression in whole brain extracts of male wild-type mice, male 'Rescue' mice and male 'Non-Rescue' mice. (**B**) Representative western blot showing Mecp2 expression in whole brain extracts of female wild-type mice, female 'Rescue' mice and female 'Non-Rescue' mice. (**C**) Histogram depicting the relative expression levels (mean $\pm$ standard error) of Mecp2 protein in whole brain homogenates derived from male 'Rescue' mice ($n = 4$) and male 'Non-Rescue' mice ($n = 5$). The values reflect the ratio of the densitometric value for MeCP2 immunoreactivity and GAPDH from the same blot, expressed as a percentage of wild-type. *Indicates statistical significance, $P < 0.05$ one-way ANOVA. (**D**) Histogram depicting the relative expression levels (mean $\pm$ standard error) of Mecp2 protein in whole brain homogenates from female 'Rescue' mice ($n = 3$) and female 'Non-Rescue' mice ($n = 3$) normalized as described above. Although a trend toward increased Mecp2 levels is apparent, the difference in the normalized Mecp2 expression levels for female 'Rescue' and female 'Non-Rescue' mice failed to reach statistical significance ($P = 0.08$, one-way ANOVA). (**E** and **F**) Immunostaining of Mecp2 expression (red channel) together with the nuclear stain DAPI in the cingulate cortex (E) and dentate gyrus (F) of a male wild-type mouse (top panels), a male 'Non-Rescue' mouse (middle panels) and a male 'Rescue' mouse (bottom panels) at 2 months following *Mecp2* gene reactivation. Scale bar denotes 100 μm.

Delayed *Mecp2* reactivation reverses acquired behavioral impairments

We then examined whether or not specific established behavioral impairments would be rescued by delayed *Mecp2* reactivation in male and female Mecp2-deficient mice, and if so to what degree. For these assessments, we examined sensory-motor functions using the open field ambulation test, balance using the accelerating rotarod test, anxiety-like behavior using the light/dark place preference test and social tendencies using the nest-building test (Fig. 3). Male 'Non-Rescue' mice were tested between 50 and 70 days of age, while male 'Rescue' mice were tested at least 2 months after tamoxifen treatment (between 100 and 120 days of age). Female 'Non-Rescue' Mecp2-deficient mice

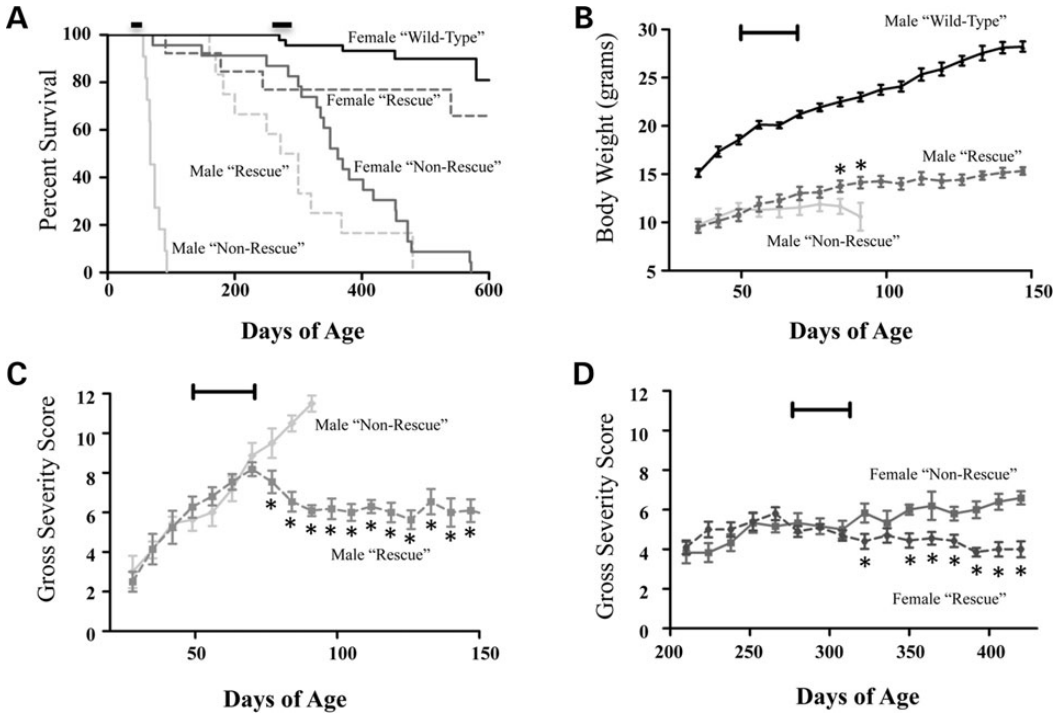

Figure 2. Restoring Mecp2 expression extends lifespan and improves gross behavior in male and female Mecp2-deficient mice. (**A**) Kaplan–Meier survival plot of wild-type mice ($n = 44$, solid black line), male 'Non-Rescue' mice ($n = 11$, solid light gray line), male 'Rescue' mice ($n = 12$, dashed light gray line), female 'Non-Rescue' mice ($n = 26$, solid dark gray line) and female 'Rescue' mice ($n = 10$, dashed dark gray line). The lifespan of male 'Rescue' mouse cohort was significantly longer than that of male 'Non-Rescue' mice ($P < 0.001$), and not significantly different from the female 'Non-Rescue' mice ($P = 0.16$). Similarly, the lifespan of the female 'Rescue' mouse cohort was significantly longer compared with female 'Non-Rescue' mice ($P < 0.01$) and was not significantly different from wild-type mice ($P = 0.21$). The thick black line at the top of the panel indicates the times of tamoxifen injection for male and female mice, respectively. (**B**) Growth curve of male wild-type ($n = 20$, solid black line), male 'Non-Rescue' mice ($n = 4–12$, dashed dark gray line) and male 'Rescue' mice ($n = 7–9$, solid light gray line). (**C**) The phenotypic severity scores of male 'Rescue' mice ($n = 7–11$ at different ages, solid light gray line) was significantly diminished in male 'Rescue' mice compared with male 'Non-Rescue' mice ($n = 4–12$ at the different ages, dashed gray line) following tamoxifen administration ($P < 0.05$). (**D**) Phenotypic severity scores of female 'Rescue' mice ($n = 10$, dashed gray line) were significantly lower than female 'Non-Rescue' mice ($n = 6$, solid gray line) following tamoxifen administration. A Wilcoxon rank-sum test with *post hoc* correction for multiple comparisons was used for statistical analysis. Data are presented as mean ± standard error, and * indicates statistical significance as denoted at $P < 0.05$.

were assessed between 9 and 14 months of age, and female 'Rescue' mice were similarly tested at least 2 months after tamoxifen treatment (11–15 months of age). These assays were conducted on independent groups, rather than on pre- versus post-tamoxifen comparisons, to maintain the novelty component for each test as appropriate.

Open-field test

In the open-field test, male 'Non-Rescue' mice exhibited a 74.2 ± 1.9% decrease in total horizontal and vertical activity counts, an 83.5 ± 2.1% decrease in total horizontal mobility counts, an 86.4 ± 2.3% decrease in total vertical rearing counts, a 95.7 ± 0.3% decrease in center rearing counts, a 40.2 ± 3.3% decrease in ambulation rate and a 76.2 ± 2.9% decrease in complete cage exploration trips when compared with age-matched male wild-type mice (Fig. 3A and B). Each value was significantly decreased from age-matched wild-type male mice. Female 'Non-Rescue' mice displayed a 51.3 ± 4.6% decrease in total activity, a 50.6 ± 5.2% decrease in total mobility, a 43.7 ± 5.9% decrease in total rearing, a 76.8 ± 5.8% decrease in center rearing, a 19.3 ± 3.1% decrease in ambulation rate and a 37.1 ± 6.7% decrease in complete cage exploration trips when compared with age-matched female wild-type mice (Fig. 3A and B). Both male 'Rescue' and female 'Rescue' mice showed significant improvements in each of these open field parameters (except complete cage trips for female 'Rescue' mice) when compared with their respective 'Non-Rescue' counterparts ($P < 0.05$ for all parameters, one-way ANOVA; Fig. 3A), although their performances mostly remained below wild-type levels for these open field paradigms. Interestingly, although the behavioral improvement for male 'Rescue' mice was not complete, their total activity, mobility, ambulation rate and cage exploration trips completed were improved to a level that did not significantly differ from female 'Non-Rescue' mice ($P > 0.05$, one-way ANOVA; Fig. 3A). This observation is in line with the level of Mecp2 expression being roughly equivalent overall between the male 'Rescue' and female 'Non-Rescue' mice (Fig. 1C and 1D).

Light–dark place preference test

In the light/dark place preference test, male 'Non-Rescue' and female 'Non-Rescue' mice displayed significantly less risk-assessment behavior than their respective wild-type controls (Fig. 3C). Although still significantly below wild-type levels, male 'Rescue' mice displayed significantly improved risk-assessment behavior when compared with male 'Non-Rescue'

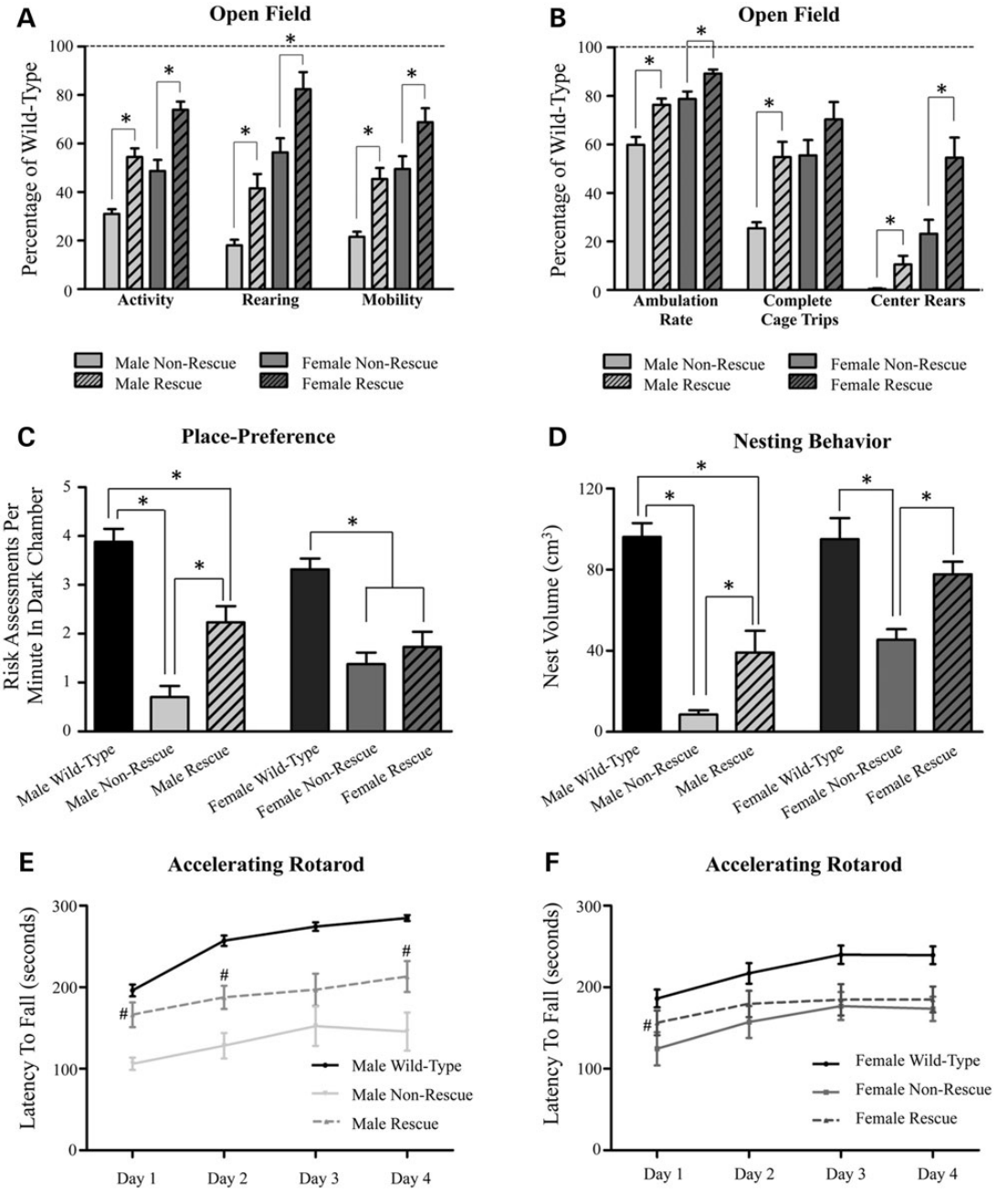

Figure 3. Growth rate, ambulation, motor coordination, anxiety and nesting building behavior were improved following *Mecp2* reactivation in male and female mice. (**A** and **B**) The open field ambulation test was used to assess total activity, total rears (vertical activity), mobility counts (horizontal activity), ambulation rate (average time per distance traveled while mobile), complete cage exploratory trips (front to rear) and center rearing (rearing at least 4 inches away from any wall of assay chamber). Each of these parameters was significantly impaired in male ($n = 20$) and female ($n = 15$) 'Non-Rescue' mice compared with wild-type ($n = 24$ males and 18 females) at the respective ages examined. Although none of these parameters was restored to wild-type levels, each was significantly improved in male 'Rescue' mice ($n = 10$), and all but complete cage exploratory trips were significantly improved in female 'Rescue' mice ($n = 9$). (**C**) Anxiety-like behavior was assessed using the light/dark preference test. Male 'Rescue' mice ($n = 7$) conducted significantly more risk assessments per minute in the dark chamber than male 'Non-Rescue' mice ($n = 6$). Female 'Rescue' mice ($n = 8$) did not show significant improvements compared with female 'Non-Rescue' mice ($n = 9$) ($P = 0.38$). (**D**) The nesting behavior test was used as an index of social cage activity. Both male ($n = 8$) and female ($n = 8$) 'Non-Rescue' mice assembled significantly smaller nests than their respective wild-type mice ($n = 13$ wild-type males and 13 wild-type females). The assembled nest volume of both male and female 'Rescue' mice ($n = 8$) was significantly larger than their respective 'Non-Rescue' mice at the same 24 h time point. (**E**) Coordinated motor performance was assessed using the accelerating rotarod test. Male 'Rescue' mice ($n = 14$) remained on the accelerating rotarod for significantly longer times than male 'Non-Rescue' mice ($n = 6$) on trial days 1, 2, and 4 ($P < 0.05$). (**F**) Female 'Rescue' mice ($n = 10$) showed significant improvement only on trial day 1 of the rotarod test compared with female 'Non-Rescue' mice ($n = 30$) ($P < 0.05$). The performance of male and female 'Non-Rescue' mice was significantly below their respective wild-type group on each trial day (not indicated). One-way ANOVA with Tukey's *post hoc* correction was used for statistical analysis of open field, light and dark place preference, and nest building test. Data are presented as mean ± standard error, and * indicates statistical significance as denoted at $P < 0.05$. Two-way ANOVA with Bonferroni's *post hoc* correction was used for statistical analysis of the accelerating rotarod. Data are presented as mean ± standard error, and # indicates statistical significance ('Rescue' versus 'Non-Rescue' for each gender) as denoted at $P < 0.05$.

mice (2.2 ± 0.3 versus 0.6 ± 0.3 risk assessments/min, respectively, $P < 0.05$, one-way ANOVA; Fig. 3C). Somewhat surprisingly, risk-assessment behavior in female 'Rescue' mice was not significantly different from that of female 'Non-Rescue' mice ($P = 0.38$, one-way ANOVA; Fig. 3C), and overall the female 'Rescue' mice conducted significantly fewer risk-assessments than wild-type females ($P < 0.05$, one-way ANOVA; Fig. 3C).

Nest-building test

In the nest-building test, male 'Non-Rescue' and female 'Non-Rescue' mice assembled nests with significantly less volume than their respective wild-type controls (3.5 ± 0.32 versus 97 ± 6.4 cm^3 for males, and 52.0 ± 6.5 versus 95.0 ± 10.4 cm^3 for females, respectively; $P < 0.01$, one-way ANOVA; Fig. 3D). Although still smaller than wild-type size, male 'Rescue' mice assembled nests with significantly larger volumes than male 'Non-Rescue' mice (37.8 ± 11.2 cm^3 for male rescue; $P < 0.05$, one-way ANOVA; Fig. 3D). As with the previous behaviors, the nest volume of the male 'Rescue' group did not significantly differ from that of female 'Non-Rescue' mice ($P = 0.61$, one-way ANOVA). Female 'Rescue' mice assembled nests (73.8 ± 7.5 cm^3) with significantly larger volume than female 'Non-Rescue' mice ($P < 0.05$), and this final volume did not significantly differ from that of female wild-type mice ($P = 0.17$, respectively, one-way ANOVA; Fig. 3D).

Accelerating rotarod test

In the accelerating rotarod test, male 'Non-Rescue' mice and female 'Non-Rescue' mice performed significantly worse on each of the four trial days when compared with their respective age-matched wild-type controls ($P < 0.05$, two-way ANOVA, Fig. 3D). Male 'Rescue' mice showed a significant improvement relative to male 'Non-Rescue' mice on trial days 1, 2 and 4 ($P < 0.01$, two-way ANOVA). Consistent with the outcomes above, the performance of male 'Rescue' mice on the accelerating rotarod did not significantly differ from that of female 'Non-Rescue' mice on any of the trial days ($P > 0.05$, two-way ANOVA). Unlike the general improvement seen in male 'Rescue' mice, however, female 'Rescue' mice only showed a significant improvement on day 1 of the rotarod trial when compared with female 'Non-Rescue' mice ($P < 0.05$, two way ANOVA) and were not significantly improved from female 'Non-Rescue' mice on the remaining trial days.

Epileptiform discharges are significantly attenuated after *Mecp2* reactivation

In addition to behavioral impairments, male and female Mecp2-deficient mice display alterations in neural network activity. One such network alteration is the presence of spontaneous epileptiform-like discharge events (19,23,34,35). To determine whether or not established neural circuitry deficits are also reversible in symptomatic Mecp2-deficient male and female mice, we compared cortical electroencephalogram (EEG) activity profiles of wild-type, 'Non-Rescue' and 'Rescue' cohorts of mice. Analysis of cohorts was required for these assessments as electrode implantation was done in the 'Rescue' mice following tamoxifen administration. No epileptiform discharge activity was detected in any of the control wild-type mice (data not shown). Male 'Non-Rescue' mice of 50 days age, however, exhibited 45 ± 8 epileptiform discharge events per hour. These discharge events had an average duration of 2.8 ± 0.7 s and an average frequency of 6.2 ± 0.3 Hz (Fig. 4A, E–G). Although epileptiform discharge events were still observed in male 'Rescue' mice at 2 months post-reactivation, the incidence rate and average duration of the events was significantly reduced from that of male 'Non-Rescue' mice. Spontaneous discharge activity in male 'Rescue' mice was found to be 21 ± 3 events per hour, with average durations of 1.0 ± 0.1 s, and an average frequency of 6.8 ± 0.2 Hz ($P < 0.05$ for each compared with 'Non-Rescue'; one-way ANOVA; Fig. 4B, E–G).

Female 'Non-Rescue' mice displayed a significantly higher discharge incidence rate than male 'Non-Rescue' mice, with an average of 76 ± 17 discharges per hour (Fig. 4E). However, the average discharge duration of female 'Non-Rescue' mice was significantly shorter than that of male 'Non-Rescue' mice (1.11 ± 0.1 s, $P < 0.05$, one-way ANOVA, Fig. 4G), and the average frequency of the female 'Non-Rescue' discharges was also significantly higher than male 'Non-Rescue' mice (7.9 ± 0.4 Hz; $P < 0.05$, one-way ANOVA; Fig. 4F). In female 'Rescue' mice, the discharge incidence rate was significantly reduced compared with female 'Non-Rescue' mice (32 ± 4 events per hour; $P < 0.05$, one-way ANOVA; Fig. 4E), but no significant changes were observed for either the discharge duration (1.2 ± 0.1 s; Fig. 4G) or for the average frequency of the discharge event (7.7 ± 0.3 Hz; Fig. 4F). Consistent with their male counterparts, female wild-type mice did not display any baseline discharge activity (data not shown).

Delayed *Mecp2* reactivation improves EEG oscillatory activity in male and female Mecp2-deficient mice

In addition to discharge activity, we have demonstrated previously that both male and female Mecp2-deficient mice display significant deficits in total hippocampal gamma band power, as well as alterations in the peak hippocampal theta frequency, during periods of behavioral exploration (23,34). Consistent with these previous observations, spectral analysis of raw EEG power in the gamma frequency band of 35–60 Hz revealed a significant decrease in total gamma power in male 'Non-Rescue' mice compared with male wild-type mice (1.4 ± 0.1 × 10^{-4} mV^2/Hz versus 2.5 ± 0.1 × 10^{-4} mV^2/Hz, respectively; $P < 0.05$, one-way ANOVA; Fig. 5D). This decrease in power was specific to the gamma band, as no significant differences in total power were noted between wild-type and male 'Non-Rescue' mice in the 1–4 Hz delta band, or in the 6–12 Hz theta band (Fig. 5E and F). Delayed *Mecp2* reactivation rescued the gamma power deficit, as total gamma band power in male 'Rescue' mice was found to be 2.4 ± 0.2 × 10^{-4} mV^2/Hz (Fig. 5D). Intriguingly, this level did not differ significantly from that of wild-type mice ($P = 0.66$). Moreover, consistent with previous observations (23,34), male 'Non-Rescue' mice also displayed a significant decrease in their peak hippocampal theta frequency during periods of behavioral exploration relative to male wild-type mice (7.3 ± 0.1 versus 8.7 ± 0.2 Hz, respectively; $P < 0.01$, $P < 0.01$, one-way ANOVA, Fig. 5C). In male 'Rescue' mice, the average peak hippocampal theta frequency observed during exploratory behavior was 8.2 ± 0.2 Hz, which was significantly higher than that of male

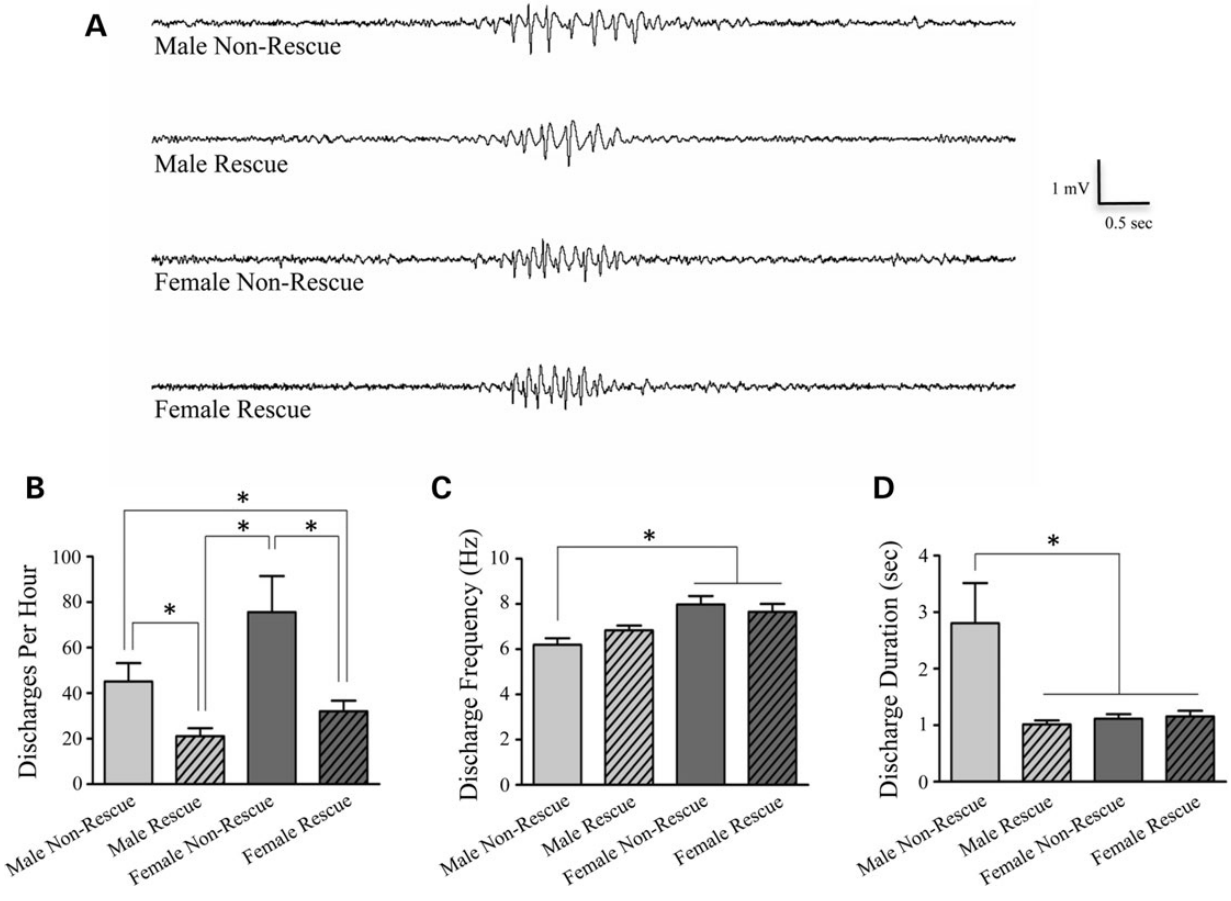

Figure 4. Cortical epileptiform discharge activity in male and female Mecp2-deficient mice is attenuated following delayed Mecp2 re-expression. (**A**) Representative 10 s traces of cortical EEG activity showing a single discharge event from a male and female 'Non-Rescue' mice, and male and female 'Rescue' mice. (**B**) The number of epileptiform discharge events per hour is significantly reduced in male 'Rescue' mice ($n = 7$) and female 'Rescue' mice ($n = 4$) compared with male 'Non-Rescue' mice ($n = 8$) and female 'Non-Rescue' mice ($n = 6$), respectively ($P < 0.01$ for both). (**C**) The average frequency of individual epileptiform discharge events was significantly slower in male 'Non-Rescue' mice ($n = 9$) compared with female 'Non-Rescue' ($n = 5$) or female 'Rescue' mice ($n = 7$). The average frequency of epileptiform discharge events of male 'Rescue' mice ($n = 7$) was not significantly different from any of the other groups ($P > 0.05$ for each). (**D**) The average duration of the remaining epileptiform discharge events in male 'Rescue' mice ($n = 7$) is significantly shorter than in male 'Non-Rescue' mice ($n = 7$), and not significantly different from either female 'Non-Rescue' mice ($n = 7$) or female 'Rescue' mice ($n = 7$). No significant differences in epileptiform discharge duration were observed between female 'Rescue' mice and female 'Non-Rescue' mice, however. No epileptiform discharge events were observed in any of the male or female wild-type mice examined ($n = 10$ for each gender). One-way ANOVA with Tukey's *post hoc* correction was used for all statistical comparisons. Data are presented as mean $\pm$ standard error, and * indicates statistical significance as denoted at $P < 0.05$.

'Non-Rescue' mice ($P < 0.05$, one-way ANOVA, Fig. 5C), and not different from the average peak theta frequency of female 'Non-Rescue' mice ($P = 0.10$, one-way ANOVA, Fig. 5C). In fact, as a group, the overall peak theta frequency in the male 'Rescue' mice did not significantly differ from that of male wild-type mice ($P = 0.21$, one-way ANOVA, Fig. 5C).

In female mice, however, there was less of an effect on peak theta frequency following *Mecp2* reactivation. Consistent with male mice, female 'Non-Rescue' mice displayed significant decreases in their peak hippocampal theta frequency during exploratory behavior compared with female wild-type mice (7.8 ± 0.2 Hz for mutants versus 8.5 ± 0.2 Hz for wild-types; $P < 0.01$, one-way ANOVA; Fig. 5B and C). In female 'Rescue' mice, the peak theta frequency was modestly improved to 8.1 ± 0.1 Hz. Although improved, this value did not reach statistical significance when compared with female 'Non-Rescue' mice ($P = 0.09$; one-way ANOVA). Consistent with male 'Non-Rescue' mice, the total gamma band power of female 'Non-Rescue' mice during exploratory behavior was reduced compared with female wild-type mice ($1.2 \pm 0.1 \times 10^{-4}$ mV^2/Hz for mutants versus $3.0 \pm 0.6 \times 10^{-4}$ mV^2/Hz for wild-type; $P < 0.05$, one-way ANOVA; Fig. 5B and D). However, the total gamma band power in female 'Rescue' mice was significantly improved to $2.7 \pm 0.5 \times 10^{-4}$ mV^2/Hz when compared with female 'Non-Rescue' mice ($P < 0.05$, one-way ANOVA), and this rescued value did not significantly differ from that of female wild-type mice ($P = 0.68$, one-way ANOVA; Fig. 5D). As with males, no differences in total EEG power were observed between female wild-type, female 'Non-Rescue' or female 'Rescue' mice in either the delta or theta bands (Fig. 5E and F).

Delayed *Mecp2* reactivation improves the home-cage activity patterns of female Mecp2-deficient mice

In addition to showing deficits in behavioral task performance, alterations in home-cage activity have also been noted in

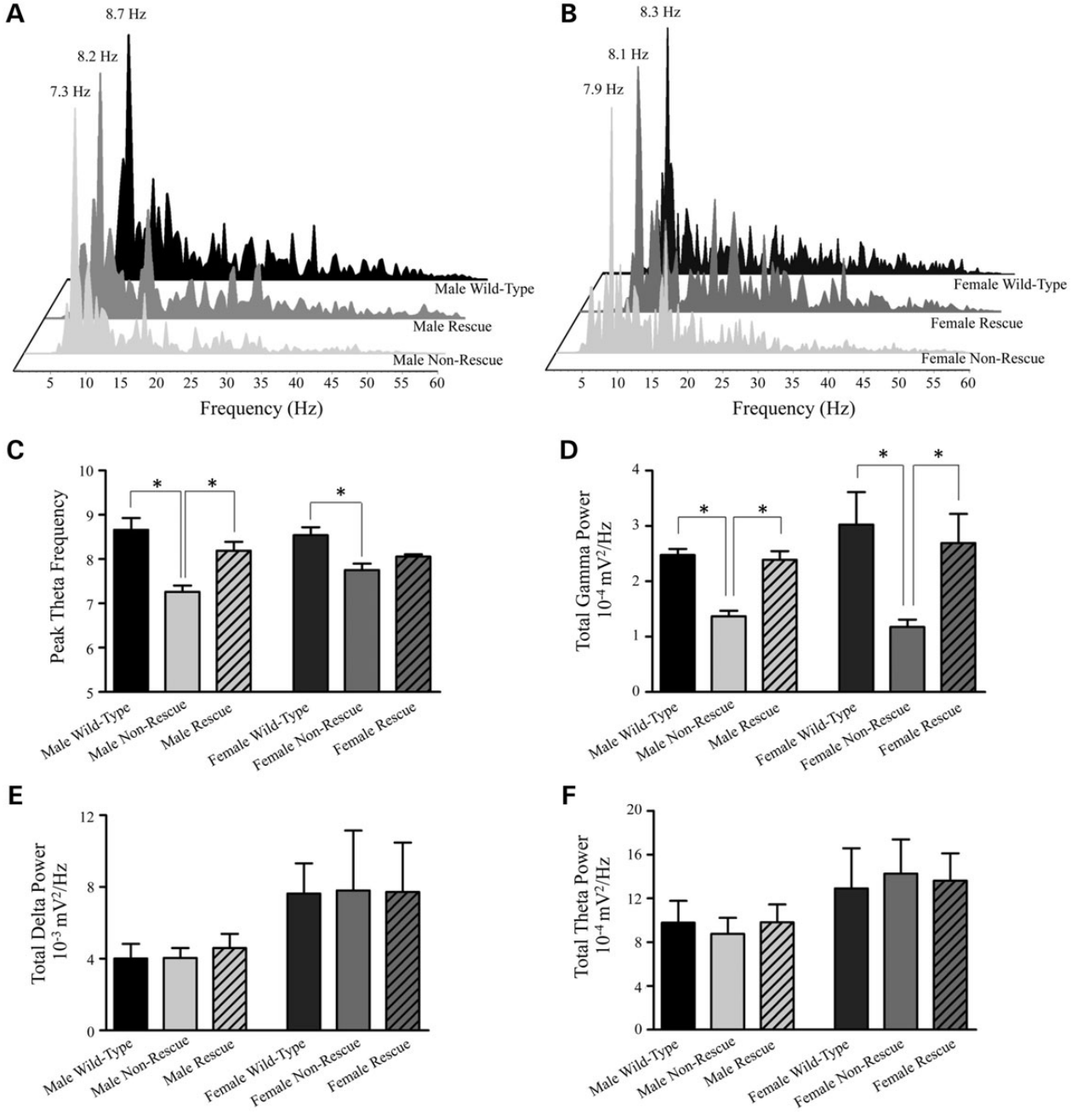

Figure 5. Restoring Mecp2 expression partially rescues peak theta frequency, and fully rescues total gamma band power in the hippocampus during exploratory behavior. (**A**) Representative power spectrum plots hippocampal EEG activity across the 5–60 Hz frequency range obtained during behavioral exploration in a male wild-type mouse, a male 'Non-Rescue' mouse and a male 'Rescue' mouse. (**B**) Representative power spectrum plots as above from a female wild-type mouse, a female 'Non-Rescue' mouse and a female 'Rescue' mouse during exploratory behavior. For (A) and (B), note the selective decrease in total gamma band power, and the shift of peak theta frequency, in the 'Non-Rescue' mice. (**C**) The peak theta frequency during exploratory behavior is significantly improved in male 'Rescue' mice ($n = 9$) compared with male 'Non-Rescue' mice ($n = 7$). However, while shifted modestly, peak theta frequency was not significantly improved in female 'Rescue' mice ($n = 5$) compared with female 'Non-Rescue' mice ($n = 8$) ($P = 0.09$ relative to 'Non-Rescue'). (**D**) Total gamma band power (35–60 Hz range) is significantly diminished from wild-type in male and female 'Non-Rescue' mice, and completely restored to wild-type levels in both male 'Rescue' ($n = 8$) and female 'Rescue' mice ($n = 5$). (E and F) No significant differences in total hippocampal delta power (**E**) or theta power (**F**) were observed between the different cohorts of male and female mice during the same exploratory behavior times examined above, illustrating the specificity of the decrease in gamma band power in the 'Non-Rescue' mice. One-way ANOVA with Tukey's *post hoc* correction was used for statistical analysis. Data are presented as mean $\pm$ standard error, and * indicates statistical significance as denoted at $P < 0.05$.

different strains of Mecp2-deficient mice (19,36). We therefore assessed whether delayed *Mecp2* reactivation in female mutants would improve aspects of their home cage behavior. For this, we employed a wireless telemetric recording system that we described previously (19) and compared behavioral patterns in female Mecp2-deficient mice before and after *Mecp2* reactivation in the same subjects. These examinations were restricted to female $Mecp2^{+/-}$ mice, as male $Mecp2^{-/y}$ mice on a pure

C57Bl/6 genetic background were not of sufficient mass for implanting the wireless transponder (19). As shown in Figure 6, the total daily home-cage activity counts, and activity counts during the light-phase and dark-phase were significantly below that of wild-type mice prior to tamoxifen administration at approximately 9 months of age. These activity counts for female wild-type were 196 ± 20 arbitrary units for total activity; 74 ± 5 arbitrary units for light phase activity; and 132 ± 12 arbitrary units for dark phase activity. In female 'Pre-Rescue' mice, these values were significantly lower, being 139 ± 9 arbitrary units for total activity; 43 ± 4 arbitrary units for light phase activity; and 96 ± 5 arbitrary units for dark phase activity; $P < 0.05$ for each, one-way ANOVA). At 2–4 months after the final tamoxifen injection of these same mice, however, their total daily home-cage activity, light-phase activity and dark-phase activity were each significantly improved compared with their pre-injection levels. These values were 207 ± 22 arbitrary units for total activity; 80 ± 11 arbitrary units for light phase activity; and 133 ± 10 arbitrary units for dark phase activity, Fig. 6. For each activity component, the performance of the 'Rescue' mice in their home cage environment did not significantly differ from wild-type levels (Fig. 6).

Delayed *Mecp2* reactivation improves thermoregulation in female Mecp2-deficient mice

It has been reported previously that daily thermoregulatory patterns are significantly altered in female Mecp2-deficient mice (19,33). Given that impaired autonomic regulation is a cornerstone feature of Rett syndrome (37,38), we assessed whether these thermoregulatory deficits would also be rescued by delayed *Mecp2* reactivation. Consistent with our previous findings (19), significant differences in daily thermoregulatory patterns were observed between wild-type and Mecp2-deficient mice. As shown in Figure 7, the daily average core body temperature of these 9-month-old female 'Pre-Rescue' mice was significantly lower than that of female wild-type controls (36.1 ± 0.1 versus 37.0 ± 0.1°C, respectively), as was their daily minimum body temperature (34.5 ± 0.1 versus 35.5 ± 0.2°C, respectively), and their daily maximum core body temperature (37.9 ± 0.1 versus 38.4 ± 0.1°C, respectively). Further, using the telemetry system to identify periods of ambulatory activity or inactivity, we found that the average core body temperature of female 'Pre-Rescue' mice was also significantly lower than that of female wild-type mice during both active (36.6 ± 0.1 versus 37.3 ± 0.1°C, respectively) and inactive (35.9 ± 0.1 versus 36.7 ± 0.1°C, respectively) behavioral periods over the 24 h day ($P < 0.01$ for both, Student's *t*-test; Fig. 7E and F). Finally, we also found that female 'Pre-Rescue' mice also displayed fewer daily temperature cycles than female wild-type mice (7.6 ± 0.7 cycles per day versus 10.0 ± 0.6 cycles per day, respectively; $P < 0.05$ one-way ANOVA). At 2–3 months following *Mecp2* reactivation, however, each of these thermoregulatory deficits in the same mutant mice was significantly improved. In these female 'Rescue' mice, the average daily core body temperature rose to 36.4 ± 0.1°C, the minimum daily core body temperature increased to 34.9 ± 0.2°C and maximum core body temperature increased to 38.3 ± 0.1°C (Fig. 7D, G, H). Similarly, the average temperature in these 'Rescue' mice was 36.9 ± 0.1°C during the active phase, and 36.2 ± 0.1°C during the inactive phase (Fig. 7E and F). Although each of these values was significantly improved from female 'Pre-Rescue' mice ($P < 0.05$, paired Student's *t*-test), the rescue was not complete, as the values remained significantly below wild-type levels (one-way ANOVA). Finally, the number of daily temperature cycles were also significantly improved in female 'Rescue' mice compared with their 'Pre-Rescue' values (10.1 ± 0.7 cycles per day; Fig. 7I), and this value was not significantly different from wild-type ($P = 0.88$; Fig. 7I).

DISCUSSION

Rett syndrome is predominately caused by mutations of the *MECP2* gene on one allele (1). Mouse models with disrupted Mecp2 expression have been generated that recapitulate many cardinal features of Rett syndrome, including motor and social impairments, altered anxiety-like responses, as well as synaptic and neural circuitry deficits (9,10,16,26,33,34,39–41). While the majority of studies to date have focused on male Mecp2-null models, heterozygous Mecp2-deficient female mice are the gender-appropriate model for the clinical disorder (9,10,17) as they express Mecp2 on average in ∼50% of their cells from early embryonic development. The male Mecp2-null model completely lacks functional Mecp2 expression, and displays a more severe gross behavioral phenotype. At the cellular level, it is important to note that while dendritic branching, neuronal packing density, nuclear volume and neuronal size are also similarly altered in Mecp2-deficient mice and Rett syndrome patients, there does not appear to be any significant neuronal degeneration resulting from the absence of Mecp2. Rather, neurons in specific brain regions appear to remain in an immature state (5,42–44), and therefore may not be irreversibly compromised. Indeed, previous work has reported that delayed near ubiquitous *Mecp2* reactivation in MeCP2-deficient mice extends lifespan, improves existing phenotypic severity, hippocampal synaptic plasticity and breathing irregularity and increases the complexity and volume of the neurons in which *Mecp2* was reactivated (16,30). However, the rescue potential for other prominent co-morbidities of Rett syndrome recapitulated in Mecp2-deficient mice remain less well examined, and particularly with respect to the gender-appropriate female Mecp2-deficient mouse model.

Consistent with previous reports (16,30), our data show that the delayed restoration of Mecp2 function has a pronounced effect on lifespan for both male and female MeCP2-deficient mice. In fact, our assessment of longevity revealed the average lifespan of female 'Rescue' mice did not significantly differ from female wild-type mice, suggesting the heightened risk of sudden and unexpected death for female Mecp2-deficient mice is completely rescued by the delayed *Mecp2* gene reactivation. While the lifespan of male 'Rescue' mice was not restored to wild-type levels, the reactivation of *Mecp2* in these mice restored MeCP2 levels to ∼50% that of wild-type, which is in essence what would be present in a female 'Non-Rescue' mice expressing Mecp2 in a random mosaic pattern. The fact that the lifespan plots of male 'Rescue' and female 'Non-Rescue' mice were not significantly different suggests a complete rescue of what might be the 'expected' lifespan of a 50% mosaic mouse, despite MeCP2 having been absent throughout

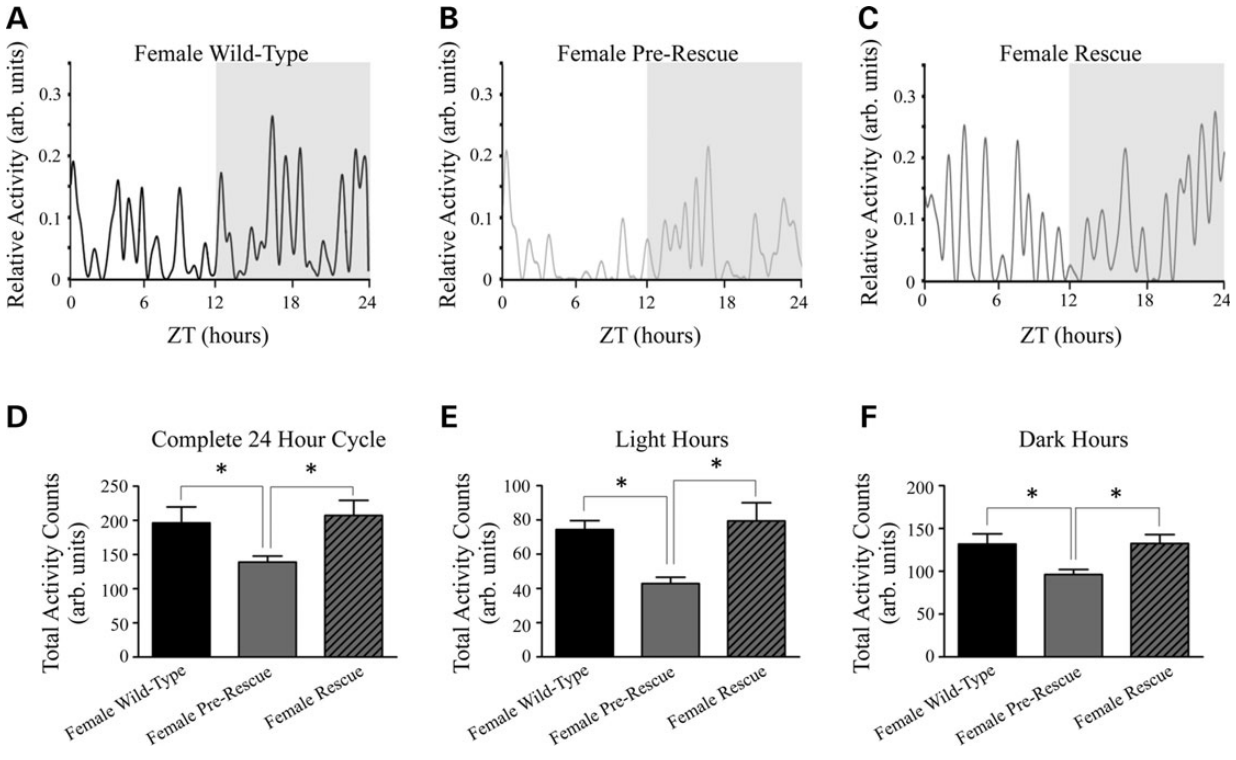

Figure 6. The delayed re-expression of Mecp2 completely rescues the daily home cage activity patterns of female Mecp2-deficient mice. (**A**–**C**) Representative 24-h home cage activity level traces of a female wild-type mouse (A), female 'Pre-Rescue' mouse (B) and the same female mouse after tamoxifen treatment (C). The dark phase of the 24-h cycle is shaded on each plot. (**D**–**F**) Histograms showing the quantitated activity counts of wild-type ($n = 8$), and the same female mutant mice 'Pre-Rescue' and 'Post-Rescue' ($n = 7$) over the entire 24-h cycle (D), and during only the light (E) or dark (F) phase of the full day. The home cage activity of 'Pre-Rescue' female Mecp2-deficient mice was significantly diminished from wild-type during both the light and dark phases of the day. Following Mecp2 re-expression, the activity of the same mice was significantly improved to wild-type levels during both the light and dark phases of the day. Paired Student's *t*-tests were used for statistical analysis of data from the same subjects 'Pre-Rescue' versus 'Post-Rescue', and one-way ANOVA with Bonferroni's *post hoc* correction was used for comparison across groups. Data are presented as mean $\pm$ standard error, and *indicates statistical significance as denoted at $P < 0.05$.

embryonic and perinatal development and being reactivated in mice at a highly symptomatic stage.

It is worth noting that these improvements occurred despite the male 'Rescue' mice remaining significantly underweighted relative to age-matched wild-type mice. While the reasons for the lack of body mass increase following *Mecp2* reactivation is not clear, and the influence of Mecp2 on body mass is clearly dependent upon the specific genetic background of the subjects (17), the lack of apparent body mass 'rescue' is not unprecedented. Using a different ubiquitously expressed estrogen receptor/cre-recombinase system than the one we employed here (32), Guy *et al*. (16) also reported a lack of body mass increase following delayed *Mecp2* reactivation in male mice on the same C57Bl/6 genetic background used for our study. Similarly, we previously found that the selective preservation of Mecp2 within the catecholaminergic system improved phenotypic impairments in male Mecp2-null mice without dramatically increasing body mass (34). In contrast, however, Ward *et al*. (33) found that preserving Mecp2 in HoxB1-expressing hindbrain neurons of Mecp2-null mice on a different genetic background did partially rescue body mass differences. As such, additional experimentation will be required to determine whether these outcomes reflect nuances of specific genetic backgrounds, or an inability of delayed Mecp2 reactivation to rescue pre-existing body mass alterations.

In addition to lifespan extension, our data also show that significant improvements in behavioral performance, cortical and hippocampal EEG activity and oscillatory patterning, and core body thermoregulation can also be achieved by delayed *Mecp2* reactivation. In fact, the performance of male 'Rescue' mice did not significantly differ from female 'Non-Rescue' mice in the open field, rotarod, place-preference or nesting behavior tests despite their absence of Mecp2 during these periods of brain development. These behavioral tasks were selected as they assess locomotive, balance, anxiety-related and social contextual behaviors in Mecp2-deficient mice that have relevance to co-morbidities seen clinically in Rett syndrome patients (17), and involve a spectrum of different neural circuitries. Collectively, our results suggest that the potential for behavioral recovery in the Mecp2-deficient neural systems that underlie these tasks is not dramatically affected by the delayed reactivation of *Mecp2*, but is rather more dependent upon the percentage of cells in which Mecp2 expression was restored. This possibility is further strengthened by the behavioral outcomes observed in female 'Rescue' mice, which on average expressed Mecp2 at 68% of wild-type levels, as their behavior in the open field and nesting behavior tasks was further improved from that of either male 'Rescue' or female 'Non-Rescue' mice. This has potential clinical relevance, as impaired ambulatory and social behavior represent major co-morbidities in most Rett syndrome

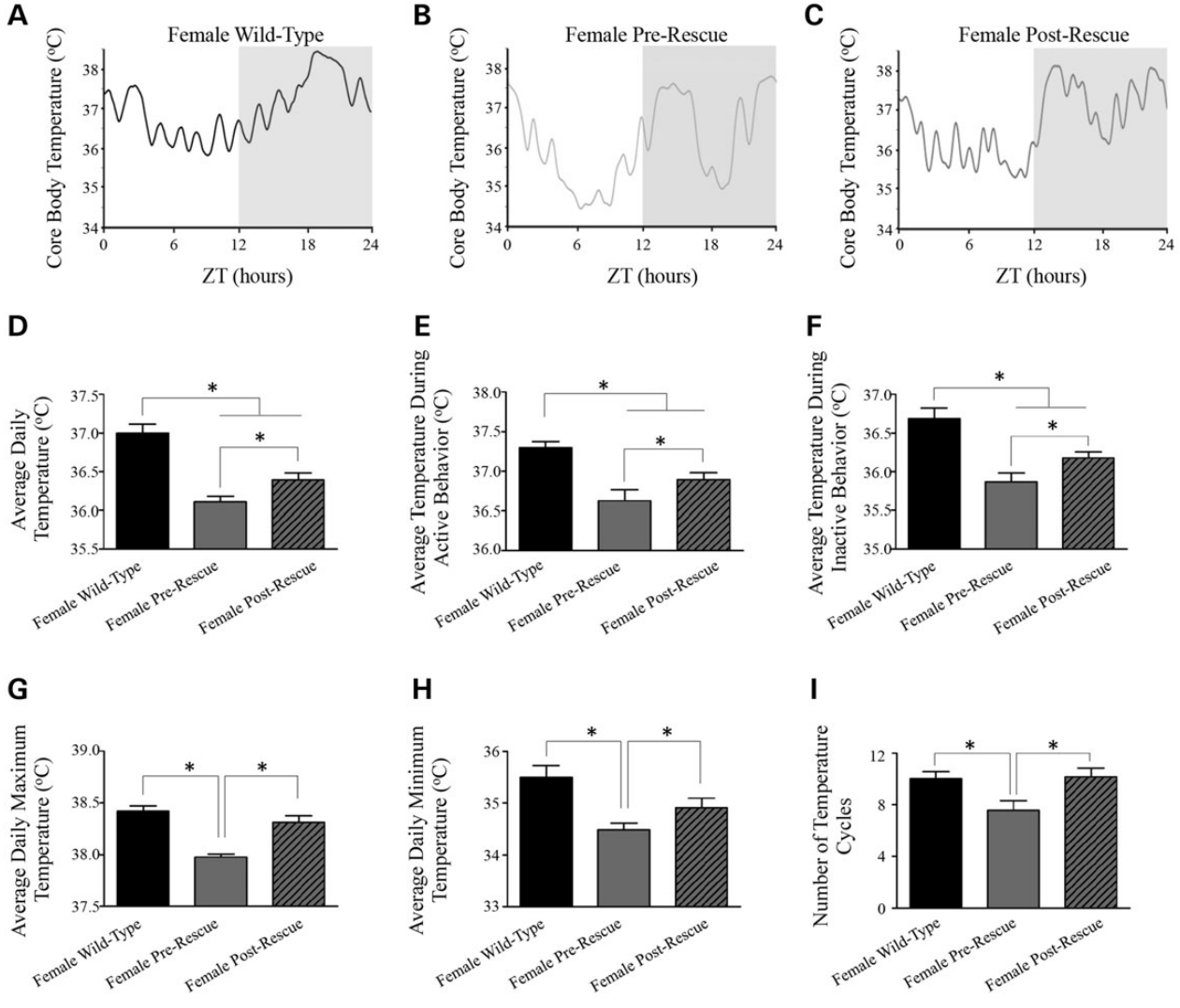

Figure 7. Thermoregulation was partially rescued in female Mecp2-deficient mice after *Mecp2* re-activation. Representative traces of the core body temperature over a complete 24-h day extracted from a female wild-type mouse (**A**), a female 'Pre-Rescue' mouse (**B**) and the same female Mecp2-deficient mouse 3 months following *Mecp2* reactivation (**C**). The shaded area on the plots denotes the dark phase of cycle. (**D**–**G**) Histograms showing the average daily body temperature (D), the average temperature during behavioral inactivity (E) and the average temperature during behavioral activity (F) of the female wild-type, female 'Pre-Rescue' and female 'Rescue' mouse cohorts. For each of these comparisons, the female 'Rescue' mouse ($n = 7$) values were significantly improved from their values in the same female mice before tamoxifen administration. Despite being improved, though, each value still remained significantly below that of the wild-type. (G and **H**) The average daily maximum body temperature (G) as well as the average daily minimum body temperature (H) of MeCP2-deficient female mice was significantly improved following *Mecp2* reactivation. For these parameters, the 'Rescue' values were not significantly different from wild-type. (**I**) The average number of daily temperature cycles was significantly improved in female 'Rescue' mice compared with female 'Pre-Rescue' ($n = 7$), and was not significantly different from the number of cycles in female wild-type mice ($n = 6$). Paired Student's *t*-tests were used for statistical analysis between female 'Pre-Rescue' and female 'Post-Rescue' mice, and one-way ANOVA with Bonferroni's *post hoc* correction was used to compare group differences. Data are presented as mean $\pm$ standard error, and *indicates statistical significance as denoted at $P < 0.05$.

patients (6,37,45). Taken together with the longevity effects, these data provide additional compelling evidence that the phenotypic consequences of Mecp2 deficiency in both male *Mecp2*$^{-/y}$ and mosaic female *Mecp2*$^{+/-}$ mice are not irremediable, and that the degree of Mecp2 restoration likely influences the magnitude of recovery.

Somewhat surprisingly, though, improvements in behavior following *Mecp2* reactivation were not observed in female mice for each of the behavioral tasks examined. Contrary to our expectations, female 'Rescue' mice showed no significant improvements in the accelerating rotarod task outside of day 1 of the trial, or in risk-assessment behavior in the place/preference test when compared with female 'Non-Rescue' mice. The reason for the lack of improvement in these behavioral tasks for female 'Rescue' mice is not clear, particularly since improvements were evident for male 'Rescue' mice in the same tests. One possibility is that the degree of *Mecp2* reactivation in the female 'Rescue' mice was not of sufficient magnitude to improve performance in these specific behaviors from the levels of mice already possessing on average a 50% Mecp2 expression profile. We attempted to correlate *Mecp2* reactivation efficiency with the degree of phenotypic improvement in these tasks, but the

sample sizes were insufficient to yield meaningful insight with the observed Mecp2 expression variance in the female subjects (data not shown). Alternatively, it is possible that because female heterozygous Mecp2-deficient mice display a less severe impairment than males for these behaviors, their performance already reaches the ceiling for recovery. The more severe phenotype of males at an earlier stage of development provides a larger window of phenotypic rescue potential. Finally, it is also possible that the age difference between *Mecp2* reactivation in the male and female 'Rescue' mice may have affected phenotypic rescue potential in these tasks. In this regard, it is worth noting that the performance of the older female wild-type mice in each of these behavioral tasks was significantly different from that of the younger male wild-type mice, suggesting gender and/or age does influence these behavioral outcomes independent of genotype. As such, this raises the possibility that the ceiling of potential rescue for these tasks in female mice may be differentially influenced by age. Consistent with this, there were clear improvements in female 'Rescue' mice in tasks where no significant differences were noted between the performance of younger male and older female wild-type mice. While not definitive, these results raise the possibility that for at least some Rett-like behavioral deficits, an earlier restoration of Mecp2 function may facilitate enhanced behavioral recovery.

One of the novel aspects of the current study was the examination of whether or not specific neural circuitry pattern impairments in the Mecp2-deficient brain can be corrected by delayed *Mecp2* reactivation. Our results support this possibility, as in addition to the improvements in behavior discussed above, delayed *Mecp2* reactivation decreased the incidence rate of spontaneous epileptiform discharge activity and improved specific alterations in behavioral state-dependent hippocampal EEG activity in both male and female 'Rescue' mice. These outcomes illustrate that the established network hyper-excitability (20,23,28,35,46), and the diminished power of neuronal network patterning systems (23,34), in Mecp2-null cortical and hippocampal circuits is not permanently engrained. These results therefore argue that the deficiency of Mecp2 function during the synaptogenesis and synaptic maturation stages does not irreversibly compromise the potential for neural circuits to achieve beneficial plasticity responses. This is consistent with recent morphological results in male 'Rescue' mice showing the attenuated neuronal complexity of Mecp2-deficient neurons increases following *Mecp2* reactivation (30), and with previous results showing hippocampal LTP levels also improve following delayed *Mecp2* reactivation (16). Collectively, these results support a model in which Mecp2-deficient networks are either stalled at an immature state, or have failed to properly mature during the normal window of synaptic development (38,42–44), but retain the potential to restructure and generate neural networks largely consistent with that of the normal mature brain following the reintroduction of functional Mecp2.

In addition to assessing behavioral performances in specific tasks and monitoring EEG activity acutely during a specific behavioral state, we also evaluated the general daily activity and thermoregulation patterns of female 'Pre-Rescue' and female 'Rescue' mice in their home-cage environment over a daily 24-h cycle. Consistent with their performance in the open field task, female 'Pre-Rescue' mice displayed hypo-activity during both the dark and light phases of the daily cycle. Unlike the partial recovery of performance seen in female 'Rescue' mice in the open field task, however, the home-cage activity observed for female 'Rescue' mice was fully returned to wild-type levels for both the dark and light phases of the day. The reason for the complete versus partial recovery in activity levels between the two assay systems is unclear, but may arise from the increased stress the animals would experience in the open field test apparatus when compared with being monitored in their home cage environment. This possibility is consistent with the outcome of the light/dark place preference test, which revealed the anxiety-like phenotype of older female Mecp2-deficient mice not significantly improved by delayed *Mecp2* reactivation, and as such could influence performance in the open field test. While additional experimentation would be required to test the validity of this possibility, these results illustrate that the degree of 'Rescue' in these types of model systems can be context-dependent, and they highlight the importance of using complementary behavioral assessment tests to fully gauge phenotypic rescue.

Moreover, the telemetric system employed also allowed us to monitor the core body temperature of the mice continually throughout the day. Autonomic nervous system dysfunction is a hallmark of clinical Rett syndrome, and hypothermia is a common co-morbidity seen in many patients (38,47,48). Consistent with previous observations (19,33), female 'Pre-Rescue' mice displayed lower average daily body temperatures, fewer and more irregular daily temperature cycling patterns, as well as lower temperatures during both the active and inactive behavioral states. In 'Rescue' mice, *Mecp2* reactivation facilitated an increase in the average daily core body temperature, an improvement of body temperature responses during the active and inactive behavioral states, a restoration of near-normal daily maximal and minimal temperatures and a complete rescue of daily temperature cycling patterns. These results illustrate that in addition to improving deficits in cortical and hippocampal circuitries, pronounced and established autonomic nervous system impairments can also be significantly improved by delayed *Mecp2* reactivation.

In summary, we show in this report that specific Rett-like deficits present in symptomatic male and female Mecp2-deficient mice can be partially or fully rescued by the delayed restoration of Mecp2 function. These results extend from previous reports (16,30,39,41,49) by illustrating functional recovery in both male and female Mecp2-deficient mice in different sets of behavioral tasks, and confirming the reversibility of impaired neural networks and autonomic nervous system alterations that stem from the absence of Mecp2. This study therefore adds to the growing body of evidence indicating Rett syndrome is not an irremediable condition.

MATERIALS AND METHODS

Animals

All experimental procedures conducted on animals were approved by local animal use committees prior to initiation, and in accordance with policies established by the Canadian Council on Animal Care. Mice were housed with littermates in a controlled facility with a 12 h light and 12 h dark cycle with food and water provided *ad libitum*. Female *Mecp2*$^{Stop/+}$ mice (*Mecp2*^{tm2Bird}, Jackson Laboratories) were crossed with male

Rosa26-Esr/Cre transgenic mice (*Gt(ROSA)26*$^{Sortm1(cre/ESR1)Tyj/J}$, Jackson Laboratories) to produce experimental genotypes. All mice were maintained on a pure C57Bl/6 background. DNA samples were prepared using the HotSHOT genomic DNA method (50) on collected punches from ear tissue. Genotypes were confirmed through polymerase chain reaction. The floxed-stop sequence in mutant mice was detected using the primer set: 5′-CTTCAGTGACAACGTCGAGC and 5′-CATTCTGCACG CTTCAAAAG-3′. The sequence for cre-recombinase was detected using the primer set: 5′-AAATGTTGCTGCTGGAT AGTTTTTACTGC-3′ and 5′-GGAAGGTGTCCAATTTACT GACCGTA-3′.

Immunoblotting and analysis

Mice were sacrificed through isoflurane overdose. Brain tissue was rapidly dissected over ice and frozen over dry ice. These tissues were homogenized in RIPA buffer (50 mM Tris−HCl, 150 mM NaCl, 1% NP-40, 2 mM EDTA, 0.5% sodium deoxycholate and 0.1% SDS) with a cocktail of protease inhibitors (Pepstatin A 2 ng/ml, PMSF 40 ng/ml, antipain 2 ng/ml, leupeptin 20 ng/ml, aprotinin 20 ng/ml and MDL28170 20 ng/ml). The homogenates are centrifuged at 12 000*g* for 5 min to remove the solid precipitate. The supernatant was collected and stored at −80°C. The Folin method was used to determine the protein concentration of the samples. Proteins were resolved with SDS polyacrylamide gel electrophoresis and transferred to a polyvinylidene fluoride membrane. The membrane was pre-hybridized with blocking solution (TRIS-buffered saline containing 0.05% Tween-20 and 5% non-fat dry milk) at room temperature for 2 h followed by hybridization with primary antibodies, anti-MeCP2 (1/1000; Cell Signaling Technology, Cat # 3456S) and anti-GAPDH (1/15 000; Cehmicon, Cat # MAB374), overnight in blocking solution. HRP-linked secondary anti-bodies, anti-rabbit (1/5000; GE Healthcare, Cat # NA934) and anti-mouse (1/5000; GE Healthcare, Cat # NA931) were applied to the membrane for 2 h at room temperature after three 20 min TBST washes. Immunoreactivity was visualized by enhanced chemiluminescence and captured on film. Protein levels were determined using densitometric analysis, using glyceraldehye dehydrogenase immunoreactivity to normalize for minor load variations between lanes. Blots were scanned and visualized using the Flour-S MultiImager. Protein band densities were determined using the Quantity One Bio-Rad analysis program.

Immunohistochemistry

Mice were sacrificed through isoflurane overdose and transcardially perfused with 0.9% NaCl saline solution followed by 2% paraformaldehyde-PBS solution. Intact brain tissue was dissected and incubated in 30% sucrose-PBS solution overnight at 4°C. The brain tissue was then dried and stored at −80°C until further assessments. For sectioning, the brain was embedded in OCT compound (Sakura, Torrance, CA, USA) and sectioned in the sagittal plane. A Leica cryostat (model Jung CM 3000, Wetzlar, Germany) was used to collect coronal sections (15 μm). For immunostaining, sections were blocked with 10% NGS + 2% BSA in 0.1% PBS-T for 1 h followed by incubation with rabbit anti-MeCP2 antibody (1:500 Cell Signaling, Cat #3456S) in 0.1% PBS-T supplemented with 2% NGS overnight at 4°C. After washing the sections using 0.1% PBS-T three times, the sections were incubated with secondary antibodies conjugated to DyLight 568 (Invitrogen, goat anti-rabbit, Cat #11011) for 1 h at room temperature in dark. The sections were then washed with PBS three times and incubated with DAPI (5 μg/ml, Roche Diagnostics, Indianapolis, IN, USA, #10236276001) for 3 min. The sections were mounted on Super Frost slides (Fisher Scientific, Oakville, Ontario, Canada) with Dako Fluorescent Mounting Media (Dako, Burlington, Ontario, Canada, Cat #S302380). Sections were imaged using a Zeiss Axioplan 2 deconvolution microscope (Carl Zeiss, Gottingen, Germany).

Tamoxifen treatment for Mecp2 reactivation

Tamoxifen (Sigma) was dissolved in corn oil (6 mg/ml) through sonication and stored at 4°C until use. Tamoxifen was administered to mice through peritoneal injection for five consecutive days at 100 mg/kg. Male 'Rescue' mice were treated with tamoxifen after phenotypic symptoms have fully developed (∼50−60 days of age with a phenotypic score of at least 5). Similarly, female 'Rescue' mice were also treated with tamoxifen after symptomatic onset. The time of the initial injection ranged from 270 to 320 days, but the injection paradigm was the same for all subjects.

Phenotype severity scoring

Animals were scored using the phenotypic severity scoring system described previously (3,16,30,34). In short, mice were scored from 0−2 into the following parameters: mobility, gait, hind-limb clasping, breathing score, tremor and general condition. A score of 0 represents the absence of symptom, 1 indicates symptom present and 2 indicates the symptom is very severe. Two genotype-blinded examiners conducted the scoring independently, and their individual values were averaged to generate each specific data point as described (34).

Behavioral testing

Animals were assessed in the open field, accelerating rotarod, light and dark preference, and nest-building tests as previously described (34,39). Briefly, for the open field ambulation test, subjects were placed in a Plexiglass cage for an hour and an automated movement detection system (AM1053 activity monitors; Linton Instruments, UK) recorded the motor activities of the animals. The parameters measured included total activity (activity in both vertical and horizontal planes), rearing (vertical plane activity), mobility (horizontal plane activity; index of total ambulatory activity), ambulation rate (average speed of horizontal plane activity crossing more than two beams), complete cage trips (number of complete cage explorations; index of mobility strength) and center rearing activity (rearing in coordinates at least 4″ from any wall; an anxiety-like behavior index). For the accelerating rotarod test (index of balance and mobility strength), subjects were placed on a rotating rod apparatus (MED Associates Inc., #ENV-575M, St. Albans, Vermont)

that accelerates at a constant rate from 3.5 to 35 rpm over a 5-min duration. A laser beam sensor detects the time at which the animals fall from the rotating beam. Trials were run three times a day for four consecutive days. Consecutive trials were separated by at least 1 h to allow the animals to recover from physical fatigue. For the light–dark place preference test (index of anxiety-like behavior), mice were placed into the open compartment of a box consisting of a dark compartment and an illuminated light compartment that are connected through a single small opening. The mice were facing the door between the compartments at the start of the test. The subjects were videotaped for 5 min and the number of risk assessments (full head traversions out of the dark compartment) performed while they were in the dark compartment was counted. For the nest-building behavior test (index of social behavior), animals were placed into a new cage containing a single piece of nestlet, and the volume of the assembled nest was measured the 24 h later. All behavioral tests were conducted between 9:00 am and 1:00 pm to minimize circadian effects. Male 'Non-Rescue' mice were assayed between 50 and 70 days of age, the same time frame during which male 'Rescue' mice are treated with tamoxifen. Male 'Rescue' mice were tested between 110 and 150 days of age, and a minimum of 6 weeks after tamoxifen treatments. Female 'Rescue' mice were assayed between 11 and 15 months of age, and at least 2 months after tamoxifen treatments. Female 'Non-Rescue' mice were assayed between 9 and 14 months of age.

Electrode implantation

Two recording systems were employed in this study. For telemetry recordings, female mice were implanted with a wireless telemetry probe TA11ETA-F10 (Data Sciences International (DSI), St Paul, MN, USA) for long duration EEG, activity and core body temperature recordings as previously described (19). Briefly, animal subjects were anesthetized under 2% isoflurane and the wireless transmitter was placed in the peritoneal cavity. The recording wire was routed via a rostral subcutaneous path and the recording electrode placed in the parietal cortex region (Bregma −0.6 mm, lateral 1.5 mm and depth 1.5 mm). A reference wire and electrode was placed at Bregma −5 mm, lateral 1 mm and depth 1.5 mm. Animals were weighted pre- and post-surgery to ensure no gross abnormalities. Animals were allowed to recover for at least 3 weeks prior to any data collection. For tethered recordings, male and female mice were implanted with electrode cap assemblies as described previously (23,34,51). Briefly, animals were anesthetized under 2–4% isoflurane through inhalation. Electrodes made from polyimide-insulated stainless steel were implanted in the hippocampal CA1 (Bregma −2.3 mm, lateral 1.7 mm and depth, 2.0 mm) and contralateral somatosensory cortex (Bregma −0.8 mm, lateral 1.8 mm and depth, 1.5 mm). A reference electrode was implanted in the frontal cortex (Bregma −3.8 mm, lateral 1.8 mm and depth 1.5 mm). Male mice were implanted between 40 and 60 days of age and female mice were implanted at ∼250 days of age. The implanted mice were allowed to recover for at least a week before any further experimentation. Baytril antibiotics (Bayer Healthcare, Toronto, Ontario, Canada) were added to the water supply 2 days before surgery and 7 days after surgery to prevent infections.

Telemetric data acquisition and data analysis

Body temperature and activity of animal subjects were collected as previously described (19). Briefly, wireless waveform data are transmitted from the telemetry probe (TA11ETA-F10) to the wireless receiver (RPC-1, DIS) and analyzed using the Data-Quest A.R.T. (DSI) software. Body temperatures were recorded from the thermosensor that is contained in wireless probe. Locomotive activity was measured by assessing the standard deviation of the wireless signal strength of the transmitter to two perpendicularly arranged receiving antennae on the RPC-1 wireless receiver. Body temperature and activity data were transmitted at 50 Hz, using a sampling rate of 250 Hz. To analyze the daily patterns of core body temperature cycling, an automated discretization process algorithm was used as described previously (19). In brief, the discretization process began by normalizing each 24-h temperature signal to have a mean of 0 and a variance of 1. Then a Gaussian-based kernel with a 50-point aperture was convolved with the normalized temperature signal to obtain the envelope of the signal. Afterwards, a threshold of 0 was applied to discretize the signal into high and low body temperature states, where each individual state had a minimum duration of 15 min. A complete cycle was defined as the combination of consecutive high and low body temperature states.

Tethered EEG data acquisition and analysis

Acute EEG recordings were collected as described previously (23,34). Briefly, the implanted electrodes were connected to two independent head stages (Model-300, AM Systems Inc., Carlsborg, WA, USA). EEG signals were amplified 1000×, bandpass filtered (0.01–1000 Hz) and digitized (Digidata 1300, Axon Instruments, Weatherford, TX, USA). EEG data were collected at 60 kHz and analyzed using Clampfit software (Axon Instruments). Recording sessions were at least 2 h long and each subject was recorded for a minimum of two sessions on different days. Cortical epileptiform discharge-like events were counted manually using the following criteria: frequency between 6–12 Hz, minimum duration of 0.5 s, at least 1.5 times the baseline amplitude and high rhythmicity. Spectral plots (50% window overlap and frequency resolution of 0.25 Hz) of hippocampal theta epochs during exploratory behavior and hippocampal delta epochs during immobile states were generated. A minimum of 10 epochs from at least two recording sessions were taken to obtain average peak theta frequency, total delta, total theta power and total gamma power for each animal. The frequency between 6–12 Hz with the greatest power was taken as the peak theta frequency. Total delta power was calculated by taking the area under the hippocampal delta spectral plot between 1and 4 Hz. Total theta power was calculated by taking the area underneath the hippocampal theta spectral plot between 6 and 12 Hz and total gamma power was taken as the area underneath the spectral plot between 35 and 60 Hz. All EEG data were calculated and analyzed using Clampfit 10.2 software.

Statistics

All statistical analysis was done using PRISM or Microsoft Excel. Wilcoxon's rank-sum test was used to analyze survival. One-way ANOVA with Bonferroni's *post hoc* correction was

used for multiple-comparisons between groups. Two-way ANOVA (genotype versus trial day) with Bonferroni's *post hoc* correction was used to analyze rotarod results. One-way ANOVA with Bonferroni's *post hoc* correction was used to compare across groups as indicated. Paired Student's *t*-tests were used as indicated to compare female 'Pre-Rescue' and 'Post-Rescue' results. Significance was set at $P < 0.05$.

ACKNOWLEDGEMENTS

We thank G. Zhang and R. Logan for technical assistance, and members of the Eubanks and Zhang laboratories for their comments on the manuscript.

Conflict of Interest statement. None declared.

FUNDING

This work was supported by the operating grants from the Canadian Institutes of Health Research to J.H.E. (MOP-106481) and B.L.B. (MOP-286154), and a proof of concept grant from the Ontario Rett Syndrome Association. M.L. was the recipient of a University of Toronto Entry Fellowship, and S.C. was the recipient of Queen Elizabeth II Graduate Scholarship in Science and Technology. Funding to pay the Open Access publication charges for this article was provided by Canadian Institutes of Health Research Grant MOP-106481.

REFERENCES

1. Amir, R.E., van den Veyver, I.B., Wan, M., Tran, C.Q., Francke, U. and Zoghbi, H.Y. (1999) Rett syndrome is caused by mutations in X-linked MECP2, encoding methyl-CpG-binding protein 2. *Nat. Genet.*, **23**, 185–188.
2. Nguyen, M.V., Du, F., Felice, C.A., Shan, X., Nigam, A., Mandel, G., Robinson, J.K. and Ballas, N. (2012) MeCP2 is critical for maintaining mature neuronal networks and global brain anatomy during late stages of postnatal brain development and in the mature adult brain. *J. Neurosci.*, **32**, 10021–10034.
3. Cheval, H., Guy, J., Merusi, C., De Sousa, D., Selfridge, J. and Bird, A. (2012) Postnatal inactivation reveals enhanced requirement for MeCP2 at distinct age windows. *Hum. Mol. Genet.*, **21**, 3806–3814.
4. McGraw, C.M., Samaco, R.C. and Zoghbi, H.Y. (2011) Adult neural function requires MeCP2. *Science*, **333**, 186.
5. Kishi, N. and Macklis, J.D. (2004) MECP2 is progressively expressed in post-migratory neurons and is involved in neuronal maturation rather than cell fate decisions. *Mol. Cell Neurosci.*, **27**, 306–321.
6. Neul, J.L. (2012) The relationship of Rett syndrome and MECP2 disorders to autism. *Dialogues Clin. Neurosci.*, **14**, 253–262.
7. Carney, R.M., Wolpert, C.M., Ravan, S.A., Shahbazian, M., Ashley-Koch, A., Cuccaro, M.L., Vance, J.M. and Pericak-Vance, M.A. (2003) Identification of MeCP2 mutations in a series of females with autistic disorder. *Pediatr. Neurol.*, **28**, 205–211.
8. Nagarajan, R.P., Hogart, A.R., Gwye, Y., Martin, M.R. and LaSalle, J.M. (2006) Reduced MeCP2 expression is frequent in autism frontal cortex and correlates with aberrant MECP2 promoter methylation. *Epigenetics*, **1**, e1–e11.
9. Guy, J., Hendrich, B., Holmes, M., Martin, J.E. and Bird, A. (2001) A mouse Mecp2-null mutation causes neurological symptoms that mimic Rett syndrome. *Nat. Genet.*, **27**, 322–326.
10. Chen, R.Z., Akbarian, S., Tudor, M. and Jaenisch, R. (2001) Deficiency of methyl-CpG binding protein-2 in CNS neurons results in a Rett-like phenotype in mice. *Nat. Genet.*, **27**, 327–331.
11. Shahbazian, M., Young, J., Yuva-Paylor, L., Spencer, C., Antalffy, B., Noebels, J., Armstrong, D., Paylor, R. and Zoghbi, H. (2002) Mice with truncated MeCP2 recapitulate many Rett syndrome features and display hyperacetylation of histone H3. *Neuron*, **35**, 243–254.
12. Pelka, G.J., Watson, C.M., Radziewic, T., Hayward, M., Lahooti, H., Christodoulou, J. and Tam, P.P. (2006) Mecp2 deficiency is associated with learning and cognitive deficits and altered gene activity in the hippocampal region of mice. *Brain*, **129**, 887–898.
13. Brendel, C., Belakhov, V., Werner, H., Wegener, E., Gärtner, J., Nudelman, I., Baasov, T. and Huppke, P. (2011) Readthrough of nonsense mutations in Rett syndrome: evaluation of novel aminoglycosides and generation of a new mouse model. *J. Mol. Med.*, **89**, 389–398.
14. Goffin, D., Allen, M., Zhang, L., Amorim, M., Wang, I.T., Reyes, A.R., Mercado-Berton, A., Ong, C., Cohen, S., Hu, L. *et al.* (2011) Rett syndrome mutation MeCP2 T158A disrupts DNA binding, protein stability and ERP responses. *Nat. Neurosci.*, **15**, 274–283.
15. Lawson-Yuen, A., Liu, D., Han, L., Jiang, Z.I., Tsai, G.E., Basu, A.C., Picker, J., Feng, J. and Coyle, J.T. (2007) Ube3a mRNA and protein expression are not decreased in Mecp2R168X mutant mice. *Brain Res.*, **1180**, 1–6.
16. Guy, J., Gan, J., Selfridge, J., Cobb, S. and Bird, A. (2007) Reversal of neurological defects in a mouse model of Rett syndrome. *Science*, **315**, 1143–1147.
17. Katz, D.M., Berger-Sweeney, J.E., Eubanks, J.H., Justice, M.J., Neul, J.L., Pozzo-Miller, L., Blue, M.E., Christian, D., Crawley, J.N., Giustetto, M. *et al.* (2012) Preclinical research in Rett syndrome: setting the foundation for translational success. *Dis. Model Mech.*, **5**, 733–745.
18. Kron, M., Howell, C.J., Adams, I.T., Ransbottom, M., Christian, D., Ogier, M. and Katz, D.M. (2012) Brain activity mapping in Mecp2 mutant mice reveals functional deficits in forebrain circuits, including key nodes in the default mode network, that are reversed with ketamine treatment. *J. Neurosci.*, **32**, 13860–13872.
19. Wither, R.G., Colic, S., Wu, C., Bardakjian, B.L., Zhang, L. and Eubanks, J.H. (2012) Daily rhythmic behaviors and thermoregulatory patterns are disrupted in adult female MeCP2-deficient mice. *PLoS ONE*, **7**, e35396.
20. Taneja, P., Ogier, M., Brooks-Harris, G., Schmid, D.A., Katz, D.M. and Nelson, S.B. (2009) Pathophysiology of locus ceruleus neurons in a mouse model of Rett syndrome. *J. Neurosci.*, **29**, 12187–12195.
21. Moretti, P., Levenson, J.M., Battaglia, F., Atkinson, R., Teague, R., Antalffy, B., Armstrong, D., Arancio, O., Sweatt, J.D. and Zoghbi, H.Y. (2006) Learning and memory and synaptic plasticity are impaired in a mouse model of Rett syndrome. *J. Neurosci.*, **26**, 319–327.
22. Dani, V.S., Chang, Q., Maffei, A., Turrigiano, G.G., Jaenisch, R. and Nelson, S.B. (2005) Reduced cortical activity due to a shift in the balance between excitation and inhibition in a mouse model of Rett syndrome. *Proc. Natl Acad. Sci. USA*, **102**, 12560–12565.
23. D'Cruz, J.A., Wu, C., Zahid, T., El-Hayek, Y., Zhang, L. and Eubanks, J.H. (2010) Alterations of cortical and hippocampal EEG activity in MeCP2-deficient mice. *Neurobiol. Dis.*, **38**, 8–16.
24. Belichenko, P.V., Oldfors, A., Hagberg, B. and Dahlstrom, A. (1994) Rett syndrome: 3-D confocal microscopy of cortical pyramidal dendrites and afferents. *Neuroreport*, **5**, 1509–1513.
25. Belichenko, P.V., Hagberg, B. and Dahlstrom, A. (1997) Morphological study of neocortical areas in Rett syndrome. *Acta Neuropath.*, **93**, 50–61.
26. Adachi, M., Autry, A.E., Covington, H.E. 3rd and Monteggia, L.M. (2009) MeCP2-mediated transcription repression in the basolateral amygdala may underlie heightened anxiety in a mouse model of Rett syndrome. *J. Neurosci.*, **29**, 4218–4227.
27. Chao, H.T., Zoghbi, H.Y. and Rosenmund, C. (2007) MeCP2 controls excitatory synaptic strength by regulating glutamatergic synapse number. *Neuron*, **56**, 58–65.
28. Zhang, L., He, J., Jugloff, D.G. and Eubanks, J.H. (2008) The MeCP2-null mouse hippocampus displays altered basal inhibitory rhythms and is prone to hyperexcitability. *Hippocampus*, **18**, 294–309.
29. Samaco, R.C., McGraw, C.M., Ward, C.S., Sun, Y., Neul, J.L. and Zoghbi, H.Y. (2013) Female Mecp2(+/−) mice display robust behavioral deficits on two different genetic backgrounds providing a framework for pre-clinical studies. *Hum. Mol. Genet.*, **22**, 96–109.
30. Robinson, L., Guy, J., McKay, L., Brockett, E., Spike, R.C., Selfridge, J., De Sousa, D., Merusi, C., Riedel, G., Bird, A. *et al.* (2012) Morphological and functional reversal of phenotypes in a mouse model of Rett syndrome. *Brain*, **135**, 2699–2710.
31. Hayashi, S. and McMahon, A.P. (2002) Efficient recombination in diverse tissues by a tamoxifen-inducible form of Cre: a tool for temporally regulated gene activation/inactivation in the mouse. *Dev. Biol.*, **244**, 305–318.

32. Ventura, A., Kirsch, D.G., McLaughlin, M.E., Tuveson, D.A., Grimm, J., Lintault, L., Newman, J., Reczek, E.E., Weissleder, R. and Jacks, T. (2007) Restoration of p53 function leads to tumour regression *in vivo*. *Nature*, **445**, 661–665.
33. Ward, C.S., Arvide, E.M., Huang, T.W., Yoo, J., Noebels, J.L. and Neul, J.L. (2011) MeCP2 is critical within HoxB1-derived tissues of mice for normal lifespan. *J. Neurosci.*, **31**, 10359–10370.
34. Lang, M., Wither, R.G., Brotchie, J.M., Wu, C., Zhang, L. and Eubanks, J.H. (2013) Selective preservation of MeCP2 in catecholaminergic cells is sufficient to improve the behavioral phenotype of male and female Mecp2-deficient mice. *Hum. Mol. Genet.*, **22**, 358–371.
35. Wither, R.G., Lang, M., Zhang, L. and Eubanks, J.H. (2013) Regional MeCP2 expression levels in the female MeCP2-deficient mouse brain correlate with specific behavioral impairments. *Exp. Neurol.*, **239**, 49–59.
36. De Filippis, B., Ricceri, L. and Laviola, G. (2010) Early postnatal behavioral changes in the Mecp2–308 truncation mouse model of Rett syndrome. *Genes Brain Behav.*, **9**, 213–223.
37. Chahrour, M. and Zoghbi, H.Y. (2007) The story of Rett syndrome: from clinic to neurobiology. *Neuron*, **56**, 422–437.
38. Roux, J.C. and Villard, L. (2010) Biogenic amines in Rett syndrome: the usual suspects. *Behav. Genet.*, **40**, 59–75.
39. Jugloff, D.G., Vandamme, K., Logan, R., Visanji, N.P., Brotchie, J.M. and Eubanks, J.H. (2008) Targeted delivery of an Mecp2 transgene to forebrain neurons improves the behavior of female Mecp2-deficient mice. *Hum. Mol. Genet.*, **17**, 1386–1396.
40. Samaco, R.C., Mandel-Brehm, C., Chao, H.T., Ward, C.S., Fyffe-Maricich, S.L., Ren, J., Hyland, K., Thaller, C., Maricich, S.M., Humphreys, P. *et al.* (2009) Loss of MeCP2 in aminergic neurons causes cell-autonomous defects in neurotransmitter synthesis and specific behavioral abnormalities. *Proc. Natl Acad. Sci. USA*, **106**, 21966–21971.
41. Lioy, D.T., Garg, S.K., Monaghan, C.E., Raber, J., Foust, K.D., Kaspar, B.K., Hirrlinger, P.G., Kirchhoff, F., Bissonnette, J.M., Ballas, N. *et al.* (2011) A role for glia in the progression of Rett's syndrome. *Nature*, **475**, 497–500.
42. Johnston, M.V., Jeon, O.H., Pevsner, J., Blue, M.E. and Naidu, S. (2001) Neurobiology of Rett syndrome: a genetic disorder of synapse development. *Brain Dev.*, **23**(Suppl. 1), S206–S213.
43. Smrt, R.D., Eaves-Egenes, J., Barkho, B.Z., Santistevan, N.J., Zhao, C., Aimone, J.B., Gage, F.H. and Zhao, X. (2007) Mecp2 deficiency leads to delayed maturation and altered gene expression in hippocampal neurons. *Neurobiol. Dis.*, **27**, 77–89.
44. Ronnett, G.V., Leopold, D., Cai, X., Hoffbuhr, K.C., Moses, L., Hoffman, E.P. and Naidu, S. (2003) Olfactory biopsies demonstrate a defect in neuronal development in Rett's syndrome. *Ann. Neurol.*, **54**, 206–218.
45. Moretti, P. and Zoghbi, H.Y. (2006) MeCP2 dysfunction in Rett syndrome and related disorders. *Curr. Opin. Genet. Dev.*, **16**, 276–281.
46. Calfa, G., Hablitz, J.J. and Pozzo-Miller, L. (2011) Network hyperexcitability in hippocampal slices from Mecp2 mutant mice revealed by voltage-sensitive dye imaging. *J. Neurophys.*, **105**, 1768–1784.
47. Naidu, S., Chatterjee, S., Murphy, M., Uematsu, S., Phillapart, M. and Moser, H. (1987) Rett syndrome: new observations. *Brain Dev.*, **9**, 525–528.
48. Weese-Mayer, D.E., Lieske, S.P., Boothby, C.M., Kenny, A.S., Bennett, H.L., Silvestri, J.M. and Ramirez, J.M. (2006) Autonomic nervous system dysregulation: breathing and heart rate perturbation during wakefulness in young girls with Rett syndrome. *Pediatr. Res.*, **60**, 443–449.
49. Giacometti, E., Luikenhuis, S., Beard, C. and Jaenisch, R. (2007) Partial rescue of MeCP2 deficiency by postnatal activation of MeCP2. *Proc. Natl Acad. Sci. USA*, **104**, 1931–1936.
50. Truett, G.E., Heeger, P., Mynatt, R.L., Truett, A.A., Walker, J.A. and Warman, M.L. (2000) Preparation of PCR-quality mouse genomic DNA with sodium hydroxide and Tris [HotShot]. *Biotechniques*, **29**, 52–54.
51. Wu, C., Wais, M., Sheppy, E., del Campo, M. and Zhang, L. (2008) A glue-based, screw-free method for implantation of intra-cranial electrodes in young mice. *J. Neurosci. Methods*, **171**, 126–131.